DRAFT VERSION APRIL 22, 2015
Preprint typeset using LaTeX style emulateapj v. 5/2/11

arXiv:1411.7354v2 [astro-ph.HE] 21 Apr 2015

TEV γ-RAY FLUXES FROM THE LONG CAMPAIGNS ON MRK421 AS CONSTRAINTS ON THE EMISSION OF TEV-PEV NEUTRINOS AND UHECRS

N. FRAIJA[1] AND A. MARINELLI [2]

(Dated: April 22, 2015)
Draft version April 22, 2015

ABSTRACT

Long TeV γ-ray campaigns have been carried out to study the spectrum, variability and duty cycle of the BL Lac object Markarian 421. These campaigns have given some evidence of the presence of protons in the jet: i) Its spectral energy distribution which shows two main peaks; one at low energies ($\sim$ 1 keV) and the other at high energies (hundreds of GeV), has been described by using synchrotron proton blazar model. ii) The study of the variability at GeV γ-rays and X-rays has indicated no significant correlation. iii) TeV γ-ray detections without activity in X-rays, called "orphan flares" have been observed in this object.
Recently, The Telescope Array Collaboration reported the arrival of 72 ultra-high-energy cosmic rays with some of them possibly related to the direction of Markarian 421. The IceCube Collaboration reported the detection of 37 extraterrestrial neutrinos in the TeV - PeV energy range collected during three consecutive years. In particular, no neutrino track events were associated with this source. In this paper, we consider the proton-photon interactions to correlate the TeV γ-ray fluxes reported by long campaigns with the neutrino and ultra-high-energy cosmic ray observations around this blazar. Considering the results reported by The IceCube and Telescope Array Collaborations, we found that only from $\sim$ 25% to 70% of TeV fluxes described with a power law function with exponential cutoff can come from the proton-photon interactions.

Subject headings: gamma rays: general – Galaxies: BL Lacertae objects individual (Markarian 421) — Physical data and processes: acceleration of particles — Physical data and processes: radiation mechanism: nonthermal

1. INTRODUCTION

At a distance of 134.1 Mpc (z=0.03), the BL Lac object Markarian 421 (Mrk 421) (de Vaucouleurs et al. 1991; Sbarufatti et al. 2005) is one of the closest known and brightest sources in the extragalactic X-ray/TeV sky. In X-rays, this object has been observed for more than 14 years, measuring fluxes ranging from few to hundreds mCrab (Isobe et al. 2010; Donnarumma et al. 2009; Niinuma et al. 2012; Krimm et al. 2009; Costa et al. 2008; Lichti et al. 2006; Balokovic et al. 2013). In particular the All-Sky Monitor (ASM) on board of the Rossi X-ray Timing Explorer (RXTE) was monitoring the X-ray sky from 1996 to 2011. This instrument observed continually the sky in four energy bands (1.5-3, 3-5, 5-12 and 1.5-12 keV) (Levine et al. 1996). The maximum X-ray flux measured was $\sim$ 4.3 counts s^{-1} which corresponds to $\sim$ 55.65 mCrab. Furthermore, Resconi et al. (2009) through RXTE/ASM data estimated the duty cycle of this source, finding a constant value of 18.1% for a standard deviation of 3σ. In TeV energies, simultaneous observations have been carried out by different telescopes based on Imaging Atmospheric Cherenkov Techniques (IACT) (Punch et al. 1992; Gaidos et al. 1996; Acciari & et al. 2011; Krennrich & et al. 2002; Albert & et al. 2007; Aharonian & et al. 2005, 2002, 2003; Carson et al. 2007; Acciari & et al. 2014) and air shower arrays (ASAs) (Bartoli & ARGO-YBJ Collaboration 2011; Abdo & et al. 2014; Amenomori & Tibet As Gamma Collaboration 2003). In particular, the Milagro experiment observed this source consecutively for a period of 906 days with a significance of 7.1 standard deviations. During these almost 3 years of observations, Milagro measured an average flux for energies above 1 TeV equal to $(0.205 \pm 0.030) \times 10^{-10}\,\mathrm{cm}^{-2}\,\mathrm{s}^{-1}$ for a spectral index of 2.3. With this observatory it was possible to estimate also the duty cycle for energies above 1 TeV for different baseline fluxes. At 3 standard deviations, the values of duty cycle reported were $\sim$ 40% and $\sim$ 27% for 0.1 Crab and 0.33 Crab of luminosity, respectively (Abdo & et al. 2014). For a period of 1.5 years (from 2008 August 5 to 2010 March 12), Mrk 421 was monitored by the Large Area Telescope (LAT) on board of the Fermi satellite. The γ-ray flux collected above 0.3 GeV was described by a power law with a photon index of 1.78 ± 0.02 and average flux of $(7.23 \pm 0.16) \times 10^{-8}\,\mathrm{ph\,cm}^{-2}\,\mathrm{s}^{-1}$ (Abdo & et al. 2010). The broadband spectral energy distribution (SED) with two peaks, one of low energy ($\sim$ 0.5 keV), and the other of high energy (at hundreds of GeV) was described through leptonic and hadronic models. In the leptonic scenario, a one-zone synchrotron self-Compton (SSC) with three accelerated electron populations (through diffusive relativistic shocks with a randomly oriented magnetic field) has been used (Finke et al. 2008; Abdo & et al. 2010). In the hadronic scenario, the peak at low energies is explained by electron synchrotron radiation whereas the high-energy peak is explained evoking the Synchrotron-Proton Blazar (SPB) model (Mücke & Protheroe 2001; Mücke et al. 2003). In addition, Abdo & et al. (2010) investigated the X-ray/GeV γ-ray correlation using RXTE/ASM and Fermi-LAT data, respectively. For RXTE/ASM, an energy range of 2-10 keV was used whereas for Fermi-LAT data two energy ranges 0.2 -2 GeV and 2 - 300 GeV were analyzed. They observed that the variability in the Fermi fluxes above 2 GeV and below 2 GeV is shorter than the variability in X-rays, and they did not find any significant correlation with X-rays in either of the two Fermi energy ranges. It is worth noting that TeV γ-ray and X-ray fluxes are usually correlated and interpreted through the standard one-zone

nifraija@astro.unam.mx and antonio.marinelli@pi.infn.it
[1] Luc Binette-Fundación UNAM Fellow. Instituto de Astronomía, Universidad Nacional Autónoma de México, Circuito Exterior, C.U., A. Postal 70-264, 04510 México D.F., México.
[2] I.N.F.N. & Physics Institute Polo Fibonacci Largo B. Pontecorvo, 3 - 56127 Pisa, Italy.

SSC model (Macomb & et al. 1995; Fossati 2008; Horan 2009), supporting a leptonic scenario. On the other hand, two unusual TeV flares without X-ray counterpart have happened (Błażejowski et al. 2005; Acciari & et al. 2011). Firstly, at around MJD 53033.4 a TeV flare was observed when the X-ray flux was low. This X-ray flux seems to have peaked 1.5 days before the γ-ray flux, and secondly, the higher TeV flux during the night of MJD 54589.21 was not accompanied by simultaneous X-ray activity. The last atypical event was interpreted in the framework of hadronic scenario (Fraija 2015).
From the above considerations, Mrk 421 may have the potential to emit high-energy neutrinos and to accelerate protons up to ultra-high energies (UHEs). Recently, The IceCube Collaboration reported the detection of 37 extraterrestrial neutrinos at 5.7σ above 30 TeV (IceCube Collaboration et al. 2013a,b; Aartsen et al. 2014). The reconstructed neutrino events in the TeV - PeV energy range have been obtained during three consecutive years of data taking (2010 to 2013). In particular, no well-located astrophysical neutrino candidates (those with muon tracks in the detector) have been associated with the location of Mrk 421. On the other hand, The Telescope Array (TA) Collaboration reported a cluster of 72 ultra-high-energy cosmic rays (UHECRs) with energies above 57 EeV. The cluster of events was centered at R. A.=146°.7, Dec.=43°.2 and had a Li-Ma statistical significance of 5.1σ within 5 years of operation. The field of view of this observatory covers the sky region above -10° of declination having a good sensitivity in the direction of Mrk 421 (Abbasi & The Telescope Array Collaboration 2014). In fact, by considering the error reported for the reconstructed directions and the deviation due to extragalactic and galactic magnetic fields, a subset of few events might be linked to the position of Mrk 421.
Taking into account the distance of Mrk 421, only 23% of the UHE proton fraction can come from this BL Lac (Kotera & Olinto 2011). Then, our starting point is to plot in a sky-map the neutrino track events detected by The IceCube Collaboration, the 72 UHECRs collected by TA experiment and the BL Lac Mrk 421. As shown in Figure 1, a circular region of 5° around Mrk 421 encloses one UHECR and no neutrino track events. In this work, we assume the presence of relativistic protons accelerated in the jet and introduce a hadronic model to link the TeV γ-ray fluxes reported by the long campaigns of the Very Energetic Radiation Imaging Telescope Array System (VERITAS, Acciari & et al. (2011)), Milagro (Abdo & et al. 2014) and Whipple (Acciari & et al. 2014) experiments with at least one UHECR observed in this region by TA experiment (Abbasi & The Telescope Array Collaboration 2014). Additionally, we link these TeV γ-ray fluxes with the absence of neutrino tracks at the TeV - PeV energy range reported by The IceCube Collaboration (IceCube Collaboration et al. 2013a; Aartsen et al. 2014). In this work we require the parameters derived from the hadronic model to be able to describe reasonably well the broadband SED of this blazar (Abdo et al. 2011). The paper is arranged as follows. In Section 2 we show a hadronic model that relates the TeV γ-ray, HE neutrinos and UHE proton fluxes through pγ interactions. In section 3 we obtain, through Monte Carlo simulation, the neutrino event rate produced by hadronic interactions and detected in a km^3 neutrino telescope on Earth. In Section 4 we discuss the capability of Mrk 421 to accelerate the UHECRs and estimate the number of expected UHECRs in the TA experiment. In Section 5 we present a full analysis and also a discussion of our results; a brief summary is given in section 6. We hereafter use primes (unprimes) to define the quantities in a comoving (observer) frame, k=$\hbar$=c=1 in natural units, and z=0.03$\simeq$ 0.

2. HADRONIC MODEL

As has been pointed out by Mücke & Protheroe (2001), relativistic protons in the jet suggest that hadronic interactions must be taken into account in describing the broadband SED, as well as neutrino emission. Relativistic protons accelerated at the emitting region and described through a power law by

$$\frac{dN_p}{dE_p} = A_p \left(\frac{E_p}{\mathrm{E_0}}\right)^{-\alpha}, \tag{1}$$

can interact with the target photon density given by

$$n_\gamma \simeq \frac{d_z^2}{r_d^2\,\epsilon_{\gamma,\mathrm{pk}}}(\nu F_\nu)\,, \tag{2}$$

where $\nu F_\nu \simeq L_\gamma/(4\pi d_z^2)$ is the photon flux, r_d is the radius of the emitting region, $\epsilon_{\gamma,\mathrm{pk}}$ is the peak energy of target photons and E_0 is the normalization proton energy. The charged (π^+) and neutral (π^0) pion production channels are $n + \pi^+$ and $p + \pi^0$, respectively. Subsequently, neutral pions decay into photons $\pi_0 \to \gamma\gamma$, and charged pions into electrons/positrons and neutrinos $\pi^\pm \to \mu^\pm + \nu_\mu/\bar{\nu}_\mu \to e^\pm + \nu_\mu/\bar{\nu}_\mu + \bar{\nu}_\mu/\nu_\mu + \nu_e/\bar{\nu}_e$.

2.1. π^0 *decay products*

From pγ interactions, photo-pions and neutrinos typically carry $10\%(\xi_{\pi^0}/2 \simeq 0.10)$ and 5% of the proton's energy E_p, respectively. The energy loss rate due to pion production can be written through the pion cooling time (Stecker 1968; Waxman & Bahcall 1997)

$$t'^{-1}_{\pi^0} = \frac{1}{2\,\gamma_p^2}\int d\epsilon\,\sigma_\pi(\epsilon)\,\xi_{\pi^0}\,\epsilon\int dx\,x^{-2}\,\frac{dn_\gamma}{d\epsilon_\gamma}(\epsilon_\gamma = x)\,, \tag{3}$$

where γ_p is the proton Lorentz factor and $\sigma_\pi(\epsilon) = \sigma_{peak} \approx 9\times 10^{-28}$ cm^2 is the cross section of pion production. Comparing the pion cooling and the dynamical time scale (photo pion efficiency), we get

$$f_{\pi^0} = \frac{t'_d}{t'_{\pi^0}} \simeq \frac{3\,L_\gamma\,\sigma_{peak}\,\Delta\epsilon_{peak}\,\xi_{\pi^0}}{4\pi\,\Gamma^2\,r_d\,\epsilon_{peak}\,\epsilon_{\gamma,\mathrm{pk}}}\begin{cases}\frac{\epsilon_{\pi^0,\gamma}}{\epsilon_{\pi^0,\gamma,c}} & \epsilon_{\pi^0,\gamma} < \epsilon_{\pi^0,\gamma,c}\\ 1 & \epsilon_{\pi^0,\gamma,c} < \epsilon_{\pi^0,\gamma}\,,\end{cases} \tag{4}$$

where $\Delta\epsilon_{peak} \simeq 0.22$ GeV and $\epsilon_{peak} \simeq 0.3$ GeV. Then, we can estimate the relation between the photo-pion and Fermi-accelerated proton fluxes as

$$f_{\pi^0}\, E_p \left(\frac{dN}{dE}\right)_p dE_p = \epsilon_{\pi^0,\gamma} \left(\frac{dN}{d\epsilon}\right)_{\pi^0,\gamma} d\epsilon_{\pi^0,\gamma}\,. \tag{5}$$

Here Γ is the bulk Lorentz factor and $\epsilon_{\pi^0,\gamma,c}$ is the break photo-pion energy. Taking into account the proton spectrum (eq. 1) and the energy fraction carried by photons, we can write the photo-pion spectrum as

$$\left(\epsilon^2 \frac{dN}{d\epsilon}\right)_{\pi^0,\gamma} = A_{p\gamma}\,\epsilon_0^2 \begin{cases} \left(\frac{\epsilon_{\pi^0,\gamma,c}}{\epsilon_0}\right)^{-1} \left(\frac{\epsilon_{\pi^0,\gamma}}{\epsilon_0}\right)^{-\alpha+3} & \epsilon_{\pi^0,\gamma} < \epsilon_{\pi^0,\gamma,c} \\ \left(\frac{\epsilon_{\pi^0,\gamma}}{\epsilon_0}\right)^{-\alpha+2} & \epsilon_{\pi^0,\gamma,c} < \epsilon_{\pi^0,\gamma}\,. \end{cases} \tag{6}$$

Here $A_{p\gamma} = b\, A_\gamma$ is obtained through the flux normalization (A_γ) of each TeV γ-ray campaign and the parameter ($0 \leq b \leq 1$) associated to the flux generated by pγ interactions. The TeV γ-ray flux is used to normalize the proton spectrum as

$$A_p \simeq f_{p,\gamma}\, A_{p\gamma} = b\, f_{p,\gamma}\, A_\gamma\,, \tag{7}$$

where $f_{p,\gamma}$ is given by

$$f_{p,\gamma} = \frac{\Gamma^2\, \epsilon_{peak} \left(\frac{2}{\xi_{\pi^0}}\right)^{\alpha-1}}{6\, r_d\, \eta_\gamma\, \sigma_{peak}\, \Delta\epsilon_{peak}}\,, \tag{8}$$

with ϵ_0 the normalization photon energy and n_γ given by eq. (2).

3. HIGH-ENERGY NEUTRINO FLUX

High-energy photons and neutrinos can be correlated through pγ interactions (Fermi-accelerated protons with keV photon targets) (see, e.g. Halzen 2007, and reference therein) as follows

$$\int \frac{dN_\nu}{dE_\nu}\, E_\nu\, dE_\nu = k_\nu \int \left(\frac{dN}{d\epsilon}\, \epsilon\, d\epsilon\right)_{\pi^0,\gamma}\,, \tag{9}$$

where k_ν is 1/4. The integral term on the right represents the TeV γ-ray flux described by eq.(6) and the term on the left is the neutrino flux which can be described as a simple power law

$$\frac{dN_\nu}{dE_\nu} = A_\nu \left(\frac{E_\nu}{\epsilon_0}\right)^{-\alpha_\nu}\,. \tag{10}$$

Here we assume that spectral indices for neutrino and γ-ray spectra are similar $\alpha \simeq \alpha_\nu$ (Becker 2008). Solving the integrals in eq. (9), we found that the normalization factors, for neutrino and photon spectrum, are related by

$$A_\nu \simeq 2^{-\alpha}\, b\, A_\gamma\,. \tag{11}$$

With these considerations, we can write the expected number of reconstructed neutrino events in a hypothetical neutrino telescope ($> E_\nu^{th}$) as

$$N_{ev} = T \rho_{w,i}\, N_A\, V_{eff} \int_{E_\nu^{th}} \sigma_{\nu N} \frac{dN_\nu}{dE_\nu}\, dE_\nu\,, \tag{12}$$

where T is the observation time, N_A=6.022$\times$ 10^{23} g^{-1} is the Avogadro number, $\rho_{w,i}$ is the density of the water/ice, $\sigma_{\nu N} = 6.78 \times 10^{-35} \mathrm{cm}^2 (E_\nu/TeV)^{0.363}$ is the neutrino-nucleon cross section (Gandhi et al. 1998) and V_{eff} is the $\nu_\mu + \bar{\nu}_\mu$ effective volume, obtained through Monte Carlo simulation for a point source emission at the position of Mrk 421. For a complete analysis, atmospheric and diffuse neutrino "backgrounds" should also be introduced. The cosmic diffuse neutrino flux is obtained with the upper limit given as $E_\nu^2\, d\Phi/dE_\nu < 2.0 \times 10^{-8}$ GeV cm^{-2}s^{-1}sr^{-1} (Bahcall & Waxman 2001) and the atmospheric neutrino flux is described by the Bartol model (Barr et al. 2006, 2004).

4. PRODUCTION OF UHE COSMIC RAYS

Astrophysical objects that accelerate cosmic rays up to UHEs, also might produce TeV γ-ray and neutrino fluxes through hadronic interactions. In our model we assume that the accelerated proton spectrum extends up to $\sim 10^{20}$ eV energies (Kachelrieß et al. 2009; Dermer et al. 2009; Protheroe et al. 2003) and based on this assumption, we calculate the number of events expected in the TA experiment.

4.1. *Hillas condition and deflexions*

Cosmic rays can be accelerated up to UHEs depending on both the size (R) and the strength of the magnetic field ($\mathcal{B}$) in the acceleration region. Therefore, the maximum energy required is $E_{max} = Ze\,\mathcal{B}\,R\,\Gamma$ with Z the atomic number (Hillas 1984). Although the Hillas criterion is a necessary condition and acceleration of UHECRs in AGN jets (Murase et al. 2012; Razzaque et al. 2012; Jiang et al. 2010), it is far from trivial (see e.g., Lemoine & Waxman 2009 for a more detailed energetics limit

(Lemoine & Waxman 2009)). Additional limitations in this process could be mainly caused by the radiative losses or available time when particles go through the magnetized region. Close to the black hole (BH), the acceleration region is limited by the emitting region (r_d) and the strength of the magnetic field (B) in it. Then, the maximum energy achieved is (Abdo & et al. 2010; Sahu et al. 2012; Fraija 2014)

$$E_{max} = Ze\,B\,r_d\,\Gamma\,. \tag{13}$$

It is worth noting that UHECRs traveling from source to Earth are randomly deviated by galactic (B_G) and extragalactic (B_{EG}) magnetic fields. By considering a quasi-constant and homogeneous magnetic field, the deflection angle due to the B_G is

$$\theta_G \simeq 3.8^\circ \left(\frac{E_{p,th}}{57EeV}\right)^{-1} \int_0^{L_G} |\frac{dl}{\mathrm{kpc}} \times \frac{B_G}{4\,\mu\mathrm{G}}|\,, \tag{14}$$

where L_G corresponds to the distance of our Galaxy (20 kpc) and due to B_{EG}, the deflection angle can be written as

$$\theta_{EG} \simeq 5^\circ \left(\frac{E_{p,th}}{57EeV}\right)^{-1} \left(\frac{B_{EG}}{1.25\,\mathrm{nG}}\right) \left(\frac{L_{EG}}{100\,\mathrm{Mpc}}\right)^{1/2} \left(\frac{l_c}{1\,\mathrm{Mpc}}\right)^{1/2}, \tag{15}$$

where l_c is the coherence length (Stanev 1997; Moharana & Gupta 2009) and $E_{p,th} = 57\,\mathrm{EeV}$ is the energy threshold of TA experiment. Due to the strength of extragalactic ($B_{EG} \simeq 1$ nG) and galactic ($B_G \simeq 4\,\mu$G) magnetic fields, UHECRs are deflected ($\psi_{EG} \simeq 5^\circ$ and $\psi_G \simeq 3.8^\circ$) between the true direction to the source, and the observed arrival direction, respectively. Evaluation of these deflection angles relates the transient UHECR sources with the high-energy neutrino and γ-ray emission.

4.2. *Expected Number of UHECRs*

The TA experiment, located at 1,400 m above sea level in Millard County (Utah), is made of three fluorescence detector (FD) stations and a scintillator surface detector (SD) array (Abu-Zayyad & et al. 2012). It was designed to observe cosmic rays that induce extensive air showers with energies above 1 EeV. This array has an area of ~ 700 km^2 and has been in operation since 2008. To estimate the number of UHECRs, we take into account the TA exposure, which for a point source is given by $\Xi\,t_{op}\,\omega(\delta_s)/\Omega$, where $\Xi\,t_{op} = (5)\,7 \times 10^2\,\mathrm{km}^2\,\mathrm{yr}$, t_{op} is the total operational time (from 2008 May 11 to 2013 May 4), $\omega(\delta_s)$ is an exposure correction factor for the declination of Mrk 421 (Sommers 2001) and $\Omega \simeq \pi$. The expected number of UHECRs above an energy $E_{p,th}$ yields

$$N_{UHECR} = F_r\,(\mathrm{TA\,Expos.}) \times\, N_p, \tag{16}$$

where F_r is the fraction of propagating cosmic rays that survives over a distance $> \mathrm{D}_z$ (Kotera & Olinto 2011) and N_p is calculated from the proton spectrum (eq. 1) extended to energies higher than $E_{p,th}$. The expected number can be written as

$$N_{UHECR} = F_r\,\frac{\Xi\,t_{op}\,\omega(\delta_s)}{\Omega\,(\alpha-1)}\,b\,f_{p,\gamma}\,A_\gamma\,\mathrm{E}_0\left(\frac{E_{p,th}}{\mathrm{E}_0}\right)^{-\alpha+1}, \tag{17}$$

with $f_{p,\gamma}$ given by eq. (8). In addition, from eqs. (1) and (7) we can compute that the proton luminosity $L_p \simeq 4\pi D_z^2\,F_r E_p^2 \frac{dN_p}{dE_p}$ can be written as

$$L_p = 4\pi D_z^2\,F_r\,b\,f_{p,\gamma}\,A_\gamma\,{\mathrm{E}_0}^2\left(\frac{E_p}{\mathrm{E}_0}\right)^{2-\alpha}. \tag{18}$$

It is worth mentioning that if $E_p = E_{p,th}$, then $L_p = L_{UHECR}$.

5. ANALYSIS AND RESULTS

We have introduced a hadronic model based on pγ interactions to describe the TeV γ-ray fluxes observed from Mrk 421. Thanks to the data collected by VERITAS telescope (Acciari & et al. 2011), Milagro observatory (Abdo & et al. 2014) and Whipple 10m telescope (Acciari & et al. 2014), we plot the light curves of Mrk 421 and fit the integrated flux over the whole time period, as shown in fig. 2. Using the method of Chi-square χ^2 minimization as implemented in the ROOT software package (Brun & Rademakers 1997), we get the integrated flux (N_γ) as reported in table 1. In this table we briefly summarize the main features of the long TeV campaigns.

Experiments	**Campaings** (Duration)	$\mathbf{T}_{live}$	$\mathbf{N}_\gamma$ ($\times 10^{-11}\,\mathrm{cm}^{-2}\,\mathrm{s}^{-1}$)
[1] VERITAS ($>$ 300 GeV)	2006 - 2008	$\simeq$ 143.3 hr	1.459 ± 0.008
[2] Milagro ($>$ 300 GeV)	2005 - 2008	$\simeq$ 900 d	1.401 ± 0.012
[3] Whipple ($>$ 400 GeV)	1995 - 2009	$\simeq$ 878.4 hr	0.495 ± 0.009

Table 1. The main features of the TeV long campaigns on Mrk 421 from 1995 to 2009. The integrated fluxes were obtained after fitting the light curves over the whole time period of observations (see fig. 2).

[1] *VERITAS.* — VERITAS is made of four 12 m diameter imaging atmospheric Cherenkov telescopes and is located at the base of the Fred Lawrence Whipple Observatory (FLWO) in south Arizona at an altitude of 1280 m. It detects γ-rays in the energy range from ~ 100 GeV to ~ 30 TeV. More details about VERITAS, the data calibration, and the analysis techniques can be found in Acciari & et al. (2008). Acciari & et al. (2011) reported observations in different states of TeV γ-ray activity between 2006 January and 2008 June. These observations for energies above 300 GeV were performed with VERITAS observatory and the Whipple 10 m telescope, 47.3 hr of VERITAS and 96 hr of Whipple.

[2] *Milagro.* — Milagro experiment, the predecessor of High Altitude Water Cherenkov (HAWC) observatory (Abeysekara & et al. 2013), was a large water-Cherenkov detector situated at the Jemez Mountains near Los Alamos, New Mexico (USA) at an altitude of 2630 m. The main detector consisted of a central 80 m $\times$ 60 m $\times$ 8 m water reservoir with 723 photomultiplier tubes (PMT) arranged in two layers (for details see Atkins et al. (2004) and Abdo & et al. (2008)). It was designed to detect TeV γ-rays at energies between 100 GeV and 100 TeV. Mrk 421 was continually observed by Milagro for a period of 906 days (between 2005 September 21 and 2008 March 15) with a significance of 7.1 standard deviations. The observed spectrum for energies above 300 GeV was consistent with previous observations performed by VERITAS (spectral index equal to 2.3 and an exponential energy cutoff between 2.2 and 5.6 TeV) (Abdo & et al. 2014).

[3] *Whipple.* — The Whipple 10m gamma-ray telescope was located at the Fred Lawrence Whipple Observatory (FLWO) in southern Arizona, USA. The predecessor of VERITAS, this telescope was in operation since 1968 and detected the first TeV gamma-ray source, the Crab Nebula in 1989 (Weekes 1996). This Telescope was sensitive in the energy range from 200 GeV to 20 TeV. More details about the descriptions of Whipple observing modes, analysis procedures and the GRANITE-III camera can be found in (Punch & Fegan 1991; Reynolds & et al. 1993; Kildea & et al 2007). Mrk 421 was studied over a 14-year time period (878.4 h, between 1995 December and May 2009) with the Whipple 10m telescope. For energies above 400 GeV, the time-average flux reported during this period was 0.446 ± 0.008 Crab flux units.

By considering the target photon flux $(\nu F_\nu)_{0.5\,\mathrm{keV}} \simeq 5 \times 10^{-10}\,\mathrm{erg\,cm^{-2}\,s^{-1}}$ (Abdo et al. 2011) and from eq. (2), it is possible to obtain a photon density equal to $n_\gamma \simeq 22.38 \times 10^{12}\,\mathrm{cm^{-3}}$. As one can see the amount of photons is copious, therefore pγ interactions become an effective process. Assuming the values reported by Abdo et al. (2011): the emitting region $r_d = 4 \times 10^{14}\,\mathrm{cm}$, the bulk Lorentz factor $\Gamma = 10$, the magnetic field $B = 50$ Gauss and the break photo-pion energy $\epsilon_{\pi^0,\gamma,c} \simeq 250\,\mathrm{GeV}$, we compute, through p$\gamma$ interactions, the neutrino flux (eq. 11), the number of UHECRs (eq. 17) and the proton luminosity (eq. 18) associated to the TeV γ-ray fluxes reported by VERITAS, Milagro and Whipple experiments. Considering a simple power law $\frac{dN_\gamma}{d\epsilon_\gamma} = A_{\gamma,\mathrm{PL}}\,(\epsilon_\gamma/\epsilon_0)^{-\alpha}$ and a power law with exponential cutoff $\frac{dN_\gamma}{d\epsilon_\gamma} = A_{\gamma,\mathrm{CPL}}\,(\epsilon_\gamma/\epsilon_0)^{-\alpha}\,\exp(-\epsilon_\gamma/\epsilon_c)$, we get the values of flux normalizations (see table 2) using the integrated fluxes reported in table 1. The values of $\mathrm{A}_{\gamma,\mathrm{PL}}$ and $\mathrm{A}_{\gamma,\mathrm{CPL}}$ are computed with the normalization energy $\epsilon_0 = \mathrm{E}_0 = 1\,\mathrm{TeV}$, the cutoff energy $\epsilon_c = 4\,\mathrm{TeV}$ and spectral index $\alpha = 2.3$ (Abdo & et al. 2014; Acciari & et al. 2011).

Experiments	$\mathbf{E}_{th}$ (TeV)	$\mathbf{A}_{\gamma,\mathrm{PL}}$ ($\times 10^{-11}\,\mathrm{TeV^{-1}\,cm^{-2}\,s^{-1}}$)	$\mathbf{A}_{\gamma,\mathrm{CPL}}$ ($\times 10^{-11}\,\mathrm{TeV^{-1}\,cm^{-2}\,s^{-1}}$)
VERITAS	0.3	3.966 ± 0.022	4.831 ± 0.027
Milagro	0.3	3.805 ± 0.033	4.636 ± 0.040
Whipple	0.4	1.955 ± 0.036	2.526 ± 0.046

Table 2. Values of the flux normalizations when we consider a simple power law $\mathrm{A}_{\gamma,\mathrm{PL}} = N_\gamma/[\int_{\epsilon_{th}} (\epsilon_\gamma/\epsilon_0)^{-\alpha}\,d\epsilon_\gamma]$ and a power law with exponential cutoff $\mathrm{A}_{\gamma,\mathrm{CPL}} = N_\gamma/[\int_{\epsilon_{th}} (\epsilon_\gamma/\epsilon_0)^{-\alpha}\,\exp(-\epsilon_\gamma/\epsilon_c)\,d\epsilon_\gamma]$. These quantities are calculated from the integrated fluxes (see table 1) and for $\epsilon_0 = 1\,\mathrm{TeV}$, $\epsilon_c = 4\,\mathrm{TeV}$ and $\alpha = 2.3$.

By assuming that HE neutrinos and TeV γ-rays are produced by pγ interactions, we use a Monte Carlo simulation to calculate the expected neutrino events per year in a hypothetical km^3 Cherenkov telescope located at the southern hemisphere. This simulation was done with the values of the spectral index, the normalization energy, the flux normalizations of the long TeV γ-ray campaigns (see table 2) and the bin of one square degree around Mrk 421 position. Figure 3 shows the neutrino event rate per year for signal and background expected from TeV γ-ray campaigns, the atmospheric and cosmic diffuse neutrino "backgrounds". Left panels in fig. 3 show the neutrino event rate per year when the TeV γ-ray fluxes are fitted with a simple power law and right panels when the TeV γ-ray fluxes are fitted with a power law with exponential cutoff for b=1.0 (top panels) and 0.7 (bottom panels). From this figure one can see that the neutrino signal begins to be higher than atmospheric neutrinos for neutrino energies above ~ 30 TeV. Then, we compute this excess of ν_μ signal above the "background" for b=1.0 and 0.7, as shown in table 3. This table shows that the neutrino events predicted in three years are 1.02, 0.96 and 0.30 (1.41, 1.35 and 0.51) when we consider b=1.0 and TeV γ-ray flux normalizations fitted with a simple power law (power law with exponential cutoff). Similarly, the neutrino events are 0.72, 0.66 and 0.21 (0.99, 0.96 and 0.30) when we take into account b=0.7 for the same TeV γ-ray flux normalizations. Taking into consideration the fact that no neutrino track events in IceCube experiment were associated to the blazar Mrk 421 during three consecutive years of data taking, we have chosen the values of b=1.0 and b=0.7 as upper limits when the long TeV

γ-ray observations have been fitted with a simple power law and a power law with exponential cutoff, respectively. We obtain that these long observations (fitted with a simple power law) could be entirely associated to the pγ interactions for the case of a simple power law fitting, whereas less than 70% (b$\leq$0.7) could be only associated to these interactions when a power law with exponential cutoff is used.

Experiments	**Neutrino events per year**			
	b=1.0		**b=0.7**	
	[a]	[b]	[a]	[b]
VERITAS	0.34	0.47	0.24	0.33
Milagro	0.32	0.45	0.22	0.32
Whipple	0.10	0.17	0.07	0.10

Table 3. Excess of ν_μ signal above the background considering a hypothetical km^3 neutrino telescope in the southern hemisphere. The labels [a] and [b] correspond to the values obtained using the TeV flux normalizations fitted with a simple power law and with a power law with exponential cutoff, respectively.

Due to extragalactic (eq. 15) and galactic (eq. 14) magnetic fields, UHECRs are deflected between the true direction to the source, and the observed arrival direction. Regarding these considerations, the total deflection angle may be as large as the mean value of $< \theta_T > \simeq 15^\circ$(Ryu et al. 2010). Therefore, it is reasonable to associate at least one UHECR within a 5° (eqs. 15) centered at Mrk 421 (see fig. 1). By assuming that the BH jet has the potential to accelerate particles up to UHEs and from eq. (13), we can see that protons at the emitting region can achieve a maximum energy of 2.37×10^{20} eV. Then, considering that proton spectrum extends up to this maximum energy (Kachelrieß et al. 2009; Dermer et al. 2009; Protheroe et al. 2003) and taking into account that 23% of proton fraction will survive over a distance of 134 Mpc (Kotera & Olinto 2011), we plot the proton luminosity normalized with the TeV fluxes fitted with a simple power law (left panels) and with a power law with exponential cutoff (right panels) for b=1.0 (top panels), 0.7 (middle panels) and 0.25 (bottom panels), as shown in Figure 4. This figure also shows two proton energies marked in blue and black colors. The blue solid line represents those protons at 10 TeV energies while the black solid line those at 57 EeV. One can see that proton luminosity is a decreasing function of proton energy and an increasing function of the parameter b. For instance, considering b=1.0 and the proton spectrum normalized with TeV fluxes fitted with a simple power law, the proton luminosity required to describe the TeV γ-ray fluxes lies in the range $3.20\times10^{44}\,\mathrm{erg/s} \leq L_p \leq 6.49\times10^{44}\,\mathrm{erg/s}$ and the UHE proton luminosity (at 57×10^{18} eV) lies in the range $3.01\times10^{42}\,\mathrm{erg/s} \leq L_p \leq 6.09\times10^{42}\,\mathrm{erg/s}$. Similarly, considering the TeV flux normalization fitted with a power law with exponential cutoff (right panels), the proton luminosity at 10 TeV lies in the range $4.14\times10^{44}\,\mathrm{erg/s} \leq L_p \leq 7.92\times10^{44}\,\mathrm{erg/s}$ and the UHE proton luminosity in the range $3.88\times10^{42}\,\mathrm{erg/s} \leq L_p \leq 7.42\times10^{42}\,\mathrm{erg/s}$. Additionally, from eq. (17) we estimate the number of events expected in TA experiment for b=1.0, 0.7 and 0.25. Table 4 shows that the number of events lie in the range $1.661 \leq N_{UHECR} \leq 3.369$ ($2.146 \leq N_{UHECR} \leq 4.104$), $1.163 \leq N_{UHECR} \leq 2.358$ ($1.502 \leq N_{UHECR} \leq 2.873$) and $0.415 \leq N_{UHECR} \leq 0.842$ ($0.537 \leq N_{UHECR} \leq 1.026$) for b=1.0, 0.7 and 0.25 when proton spectrum is normalized with TeV fluxes fitted with a simple power law (power law with exponential cutoff), respectively. One can see that the number of predicted events is higher than one for b $\geq$ 0.3 (0.25) and the proton spectrum normalized with TeV fluxes fitted with a simple power law (power law with exponential cutoff).

Experiments	**Campaigns**	**N$_{UHECR}$**					
	(Duration)	**b=1.0**		**b=0.7**		**b=0.25**	
		[a]	[b]	[a]	[b]	[a]	[b]
VERITAS	2006 - 2008	3.369 ± 0.019	4.104 ± 0.023	2.358 ± 0.013	2.873 ± 0.016	0.842 ± 0.005	1.026 ± 0.006
Milagro	2005 - 2008	3.233 ± 0.028	3.939 ± 0.034	2.263 ± 0.020	2.758 ± 0.024	0.808 ± 0.007	0.985 ± 0.009
Whipple	1995 - 2009	1.661 ± 0.031	2.146 ± 0.039	1.163 ± 0.022	1.502 ± 0.027	0.415 ± 0.008	0.537 ± 0.010

Table 4. Number of UHE protons to be expected in TA experiment. These estimations were computed through the pγ interactions and normalized with the TeV γ-ray flux fitted with a simple power law ([a]) and with a power law with exponential cutoff ([b]).

6. RESULTS AND CONCLUSIONS

We have introduced a hadronic model through pγ interactions to describe the long TeV γ-ray campaigns of the BL Lac Mrk 421 and to correlate them with the expected HE neutrino and UHECR fluxes around Mrk 421. First of all, we have obtained the integrated fluxes over the whole time period of long TeV observations performed by VERITAS, Milagro and Whipple experiments (fig. 2). Considering a simple power law and a power law with exponential cutoff we have computed the flux normalizations for

$\epsilon_0 = 1\,\mathrm{TeV}$, $\epsilon_c = 4\,\mathrm{TeV}$ and $\alpha = 2.3$ (Abdo & et al. 2014; Acciari & et al. 2011), as shown in table 2.
Correlating the TeV γ-ray and HE neutrino fluxes through pγ interactions, we have plotted (through MC simulation) the neutrino event rate per year expected from the TeV γ-ray campaigns, the atmospheric and the cosmic diffuse neutrino "backgrounds", assuming a hypothetical km^3 Cherenkov telescope in the southern hemisphere. Considering the neutrino energies $E_\nu \geq 30$ TeV for which the signal is higher than atmospheric neutrinos, we estimated the neutrino events expected in a hypothetical km^3, as shown in table 3. Taking into consideration the neutrino observations reported by The IceCube Collaboration during three consecutive years (Aartsen et al. 2014), we found that the long TeV γ-ray flux is consistent with production by pγ interactions when these observations are fitted with a simple power law and less than 70% (b$\leq$0.7) when they are fitted with a power law with exponential cutoff.
Taking into account the maximum energy achieved by Fermi-accelerated protons at the emitting region (2.7×10^{20} eV) and the TA exposure, we normalized the proton spectrum with the long TeV observations (eq. 7) in order to estimate the number of UHECRs above 57 EeV, as shown in table 4. Assuming that at least one UHECR was detected by TA experiment around the Mrk 421 position, we found that more than 30% (b$\geq$0.3) of the long TeV γ-ray observations could be associated to the pγ interactions when these observations are fitted with a simple power law and more than 25% (b$\geq$0.25) when they are fitted with a power law with exponential cutoff.
After comparing the TeV γ-ray fluxes collected from Mrk 421 with the neutrino and UHECR fluxes through pγ interactions, we conclude that only from $\sim 25\%$ to 70% of TeV γ-ray fluxes described with a power law with exponential cutoff can come from the pγ interactions and more than 30% when these observations are described with a simple power law. It is worth noting that the increasing statistics of IceCube and TA experiments will give more evidence of the presented scenario.
Considering pγ interactions to correlate the TeV γ-ray fluxes with the neutrino and UHECRs reported by IceCube and Telescope Array experiments, a lepto-hadronic model might be consistent with the observations, but it is not required.

ACKNOWLEDGEMENTS

We thank the anonymous referee for a critical reading of the paper and valuable suggestions that helped improve the quality and clarity of this work. We also thank to Francis Halzen, Ignacio Taboada, Teresa Montarulli, Patrick Moriarty and William Lee for useful discussions, Matthias Beilicke, Patrick Moriarty and Barbara Patricelli for sharing with us the data. Also we thank to TOPCAT team for the useful sky-map tools. This work was supported by Luc Binette scholarship, Galilei postdoctoral grant and the projects IG100414.

REFERENCES

Aartsen, M. G., Ackermann, M., Adams, J., et al. 2014, ArXiv e-prints, arXiv:1405.5303
Abbasi, R. U., & The Telescope Array Collaboration. 2014, ArXiv e-prints, arXiv:1404.5890
Abdo, A. A., & et al. 2008, ApJ, 688, 1078
—. 2010, ApJ, 719, 1433
—. 2014, ApJ, 782, 110
Abdo, A. A., Ackermann, M., Ajello, M., et al. 2011, ApJ, 736, 131
Abeysekara, A. U., & et al. 2013, Astroparticle Physics, 50, 26
Abu-Zayyad, T., & et al. 2012, Nuclear Instruments and Methods in Physics Research A, 689, 87
Acciari, V. A., & et al. 2008, ApJ, 679, 1427
—. 2011, ApJ, 738, 25
—. 2014, Astroparticle Physics, 54, 1
Aharonian, F., & et al. 2002, A&A, 393, 89
—. 2003, A&A, 410, 813
—. 2005, A&A, 437, 95
Albert, J., & et al. 2007, ApJ, 663, 125
Amenomori, M., & Tibet As Gamma Collaboration. 2003, ApJ, 598, 242
Atkins, R., , & et al. 2004, ApJ, 608, 680
Bahcall, J., & Waxman, E. 2001, Phys. Rev. D, 64, 023002
Balokovic, M., Furniss, A., Madejski, G., & Harrison, F. 2013, The Astronomer's Telegram, 4974, 1
Barr, G. D., Gaisser, T. K., Lipari, P., Robbins, S., & Stanev, T. 2004, Phys. Rev. D, 70, 023006
Barr, G. D., Robbins, S., Gaisser, T. K., & Stanev, T. 2006, Phys. Rev. D, 74, 094009
Bartoli, B., & ARGO-YBJ Collaboration. 2011, ApJ, 734, 110
Becker, J. K. 2008, Phys. Rep., 458, 173
Błażejowski, M., Blaylock, G., Bond, I. H., et al. 2005, ApJ, 630, 130
Brun, R., & Rademakers, F. 1997, Nuclear Instruments and Methods in Physics Research A, 389, 81
Carson, J. E., Kildea, J., Ong, R. A., et al. 2007, ApJ, 662, 199
Costa, E., Del Monte, E., Donnarumma, I., et al. 2008, The Astronomer's Telegram, 1574, 1
de Vaucouleurs, G., de Vaucouleurs, A., Corwin, Jr., H. G., et al. 1991, Third Reference Catalogue of Bright Galaxies. Volume I: Explanations and references. Volume II: Data for galaxies between 0^h and 12^h. Volume III: Data for galaxies between 12^h and 24^h.
Dermer, C. D., Razzaque, S., Finke, J. D., & Atoyan, A. 2009, New Journal of Physics, 11, 065016
Donnarumma, I., Vittorini, V., Vercellone, S., et al. 2009, ApJ, 691, L13
Finke, J. D., Dermer, C. D., & Böttcher, M. 2008, ApJ, 686, 181
Fossati, G. e. a. 2008, ApJ, 677, 906
Fraija, N. 2014, ApJ, 783, 44
—. 2015, ArXiv e-prints, arXiv:1501.04165
Gaidos, J. A., Akerlof, C. W., Biller, S., et al. 1996, Nature, 383, 319
Gandhi, R., Quigg, C., Reno, M. H., & Sarcevic, I. 1998, Phys. Rev. D, 58, 093009
Halzen, F. 2007, Ap&SS, 309, 407
Hillas, A. M. 1984, ARA&A, 22, 425
Horan, D. a. 2009, ApJ, 695, 596
IceCube Collaboration, Aartsen, M. G., Abbasi, R., et al. 2013a, ArXiv e-prints, arXiv:1311.5238
—. 2013b, ArXiv e-prints, arXiv:1304.5356
Isobe, N., Sugimori, K., Kawai, N., et al. 2010, PASJ, 62, L55
Jiang, Y.-Y., Hou, L. G., Han, J. L., Sun, X. H., & Wang, W. 2010, ApJ, 719, 459
Kachelrieß, M., Ostapchenko, S., & Tomàs, R. 2009, New Journal of Physics, 11, 065017
Kildea, J., & et al. 2007, Astroparticle Physics, 28, 182
Kotera, K., & Olinto, A. V. 2011, ARA&A, 49, 119
Krennrich, F., & et al. 2002, ApJ, 575, L9
Krimm, H. A., Barthelmy, S. D., Baumgartner, W., et al. 2009, The Astronomer's Telegram, 2292, 1
Lemoine, M., & Waxman, E. 2009, J. Cosmology Astropart. Phys., 11, 9
Levine, A. M., Bradt, H., Cui, W., et al. 1996, ApJ, 469, L33
Lichti, G. G., Paltani, S., Mowlavi, M., et al. 2006, The Astronomer's Telegram, 848, 1
Macomb, D. J., & et al. 1995, ApJ, 449, L99
Moharana, R., & Gupta, N. 2009, J. Cosmology Astropart. Phys., 8, 5
Mücke, A., & Protheroe, R. J. 2001, Astroparticle Physics, 15, 121
Mücke, A., Protheroe, R. J., Engel, R., Rachen, J. P., & Stanev, T. 2003, Astroparticle Physics, 18, 593
Murase, K., Dermer, C. D., Takami, H., & Migliori, G. 2012, ApJ, 749, 63
Niinuma, K., Kino, M., Nagai, H., et al. 2012, ApJ, 759, 84
Protheroe, R. J., Donea, A.-C., & Reimer, A. 2003, Astroparticle Physics, 19, 559

Punch, M., & Fegan, D. J. 1991, in American Institute of Physics Conference Series, Vol. 220, High Energy Gamma Ray Astronomy, ed. J. Matthews, 321–328
Punch, M., Akerlof, C. W., Cawley, M. F., et al. 1992, Nature, 358, 477
Razzaque, S., Dermer, C. D., & Finke, J. D. 2012, ApJ, 745, 196
Resconi, E., Franco, D., Gross, A., Costamante, L., & Flaccomio, E. 2009, A&A, 502, 499
Reynolds, P. T., & et al. 1993, ApJ, 404, 206
Ryu, D., Das, S., & Kang, H. 2010, ApJ, 710, 1422
Sahu, S., Zhang, B., & Fraija, N. 2012, Phys. Rev. D, 85, 043012
Sbarufatti, B., Treves, A., & Falomo, R. 2005, ApJ, 635, 173
Sommers, P. 2001, Astroparticle Physics, 14, 271
Stanev, T. 1997, ApJ, 479, 290
Stecker, F. W. 1968, Phys. Rev. Lett., 21, 1016
Waxman, E., & Bahcall, J. 1997, Phys. Rev. Lett., 78, 2292
Weekes, T. C. 1996, Space Sci. Rev., 75, 1

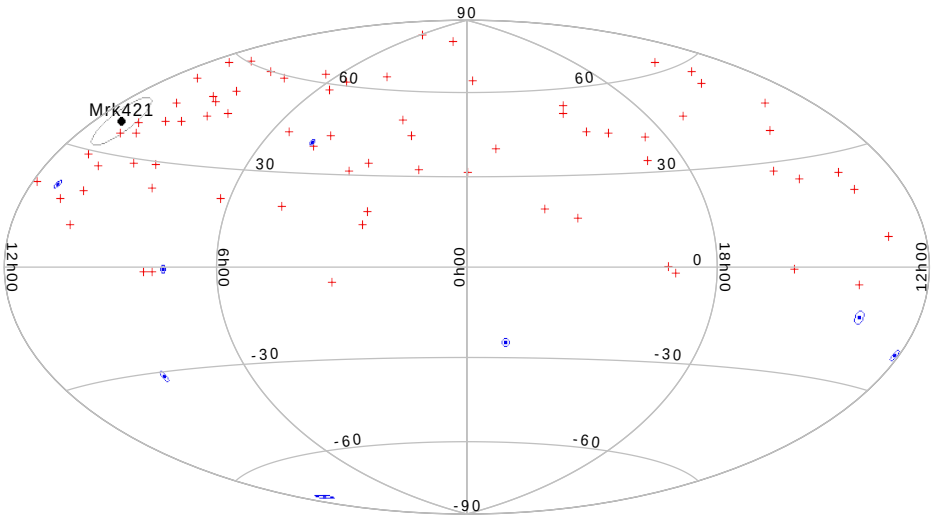

FIG. 1.— Sky-map with the 8 VHE neutrino track events detected by IceCube (blue circles), 72 UHECRs collected by TA experiments (red crosses) and the BL Lac Mrk 421 (black point).

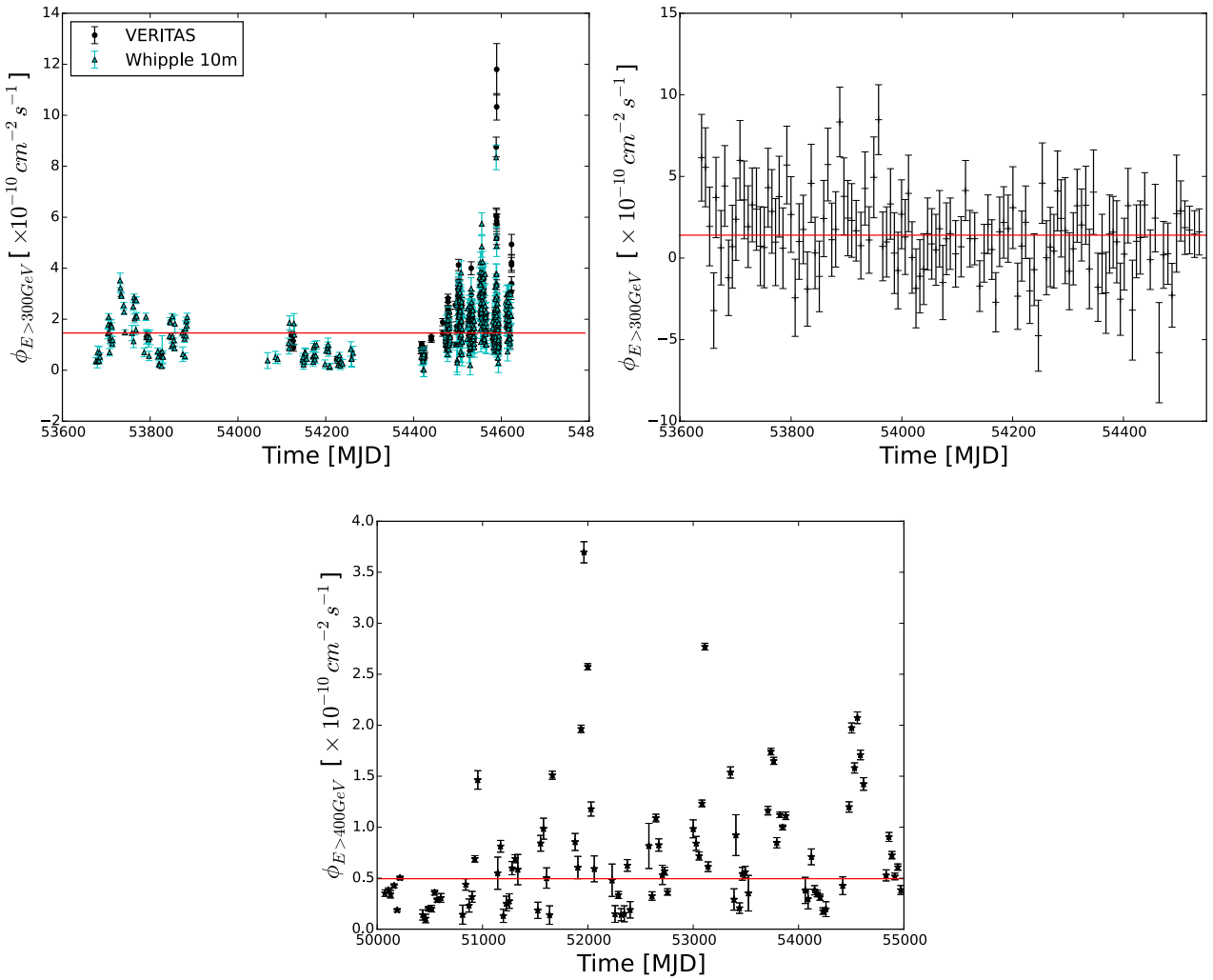

FIG. 2.— Mrk 421 light curves from the long campaigns measured by TeV γ-ray experiments. Left-hand panel above: The data consists of 47.3 hr of VERITAS and 96 hr of Whipple 10m telescope ($>$ 300 GeV) acquired between 2006 January and 2008 June. Right-hand panel above: The data consists of 3 years (between 2005 September 21 and 2008 March 15) of observation with Milagro experiment ($>$ 300 GeV). Panel below: The data consists of 14 years (878.4 h) of observation with Whipple 10m telescope ($>$ 400 GeV).

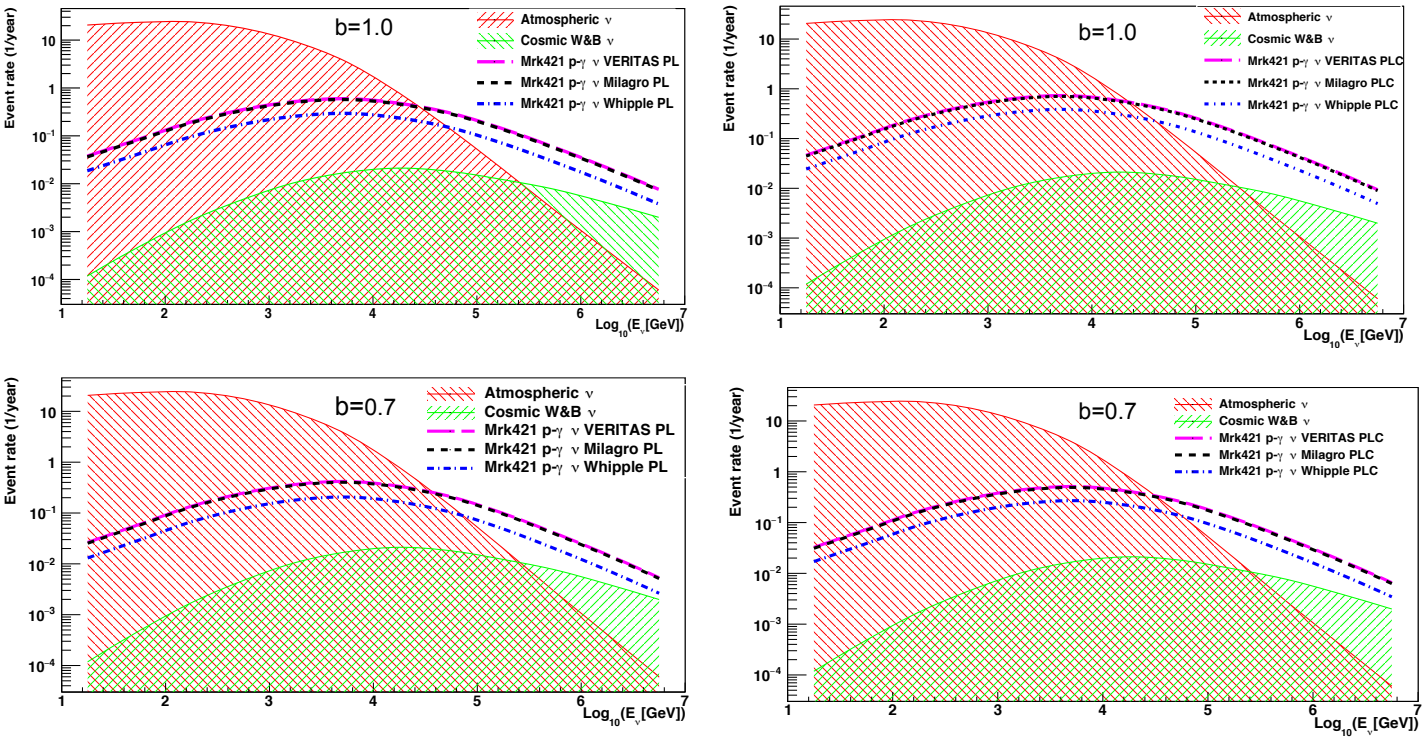

FIG. 3.— Mrk 421 neutrino event rate is plotted as a function of neutrino energy. We report the neutrino event rate per year for signal and background, for a hypothetical km^3 neutrino telescope in the south hemisphere. We normalize the neutrino event rate with the flux normalizations of the TeV γ-ray observations of Mrk 421 when a simple power law (left panel) and a power law with exponential cutoff (right panel) are considered. The long TeV campaigns, the atmospheric and the cosmic neutrino "background" are given in the plot labels. The parameter b is associated to the flux generated by pγ interactions.

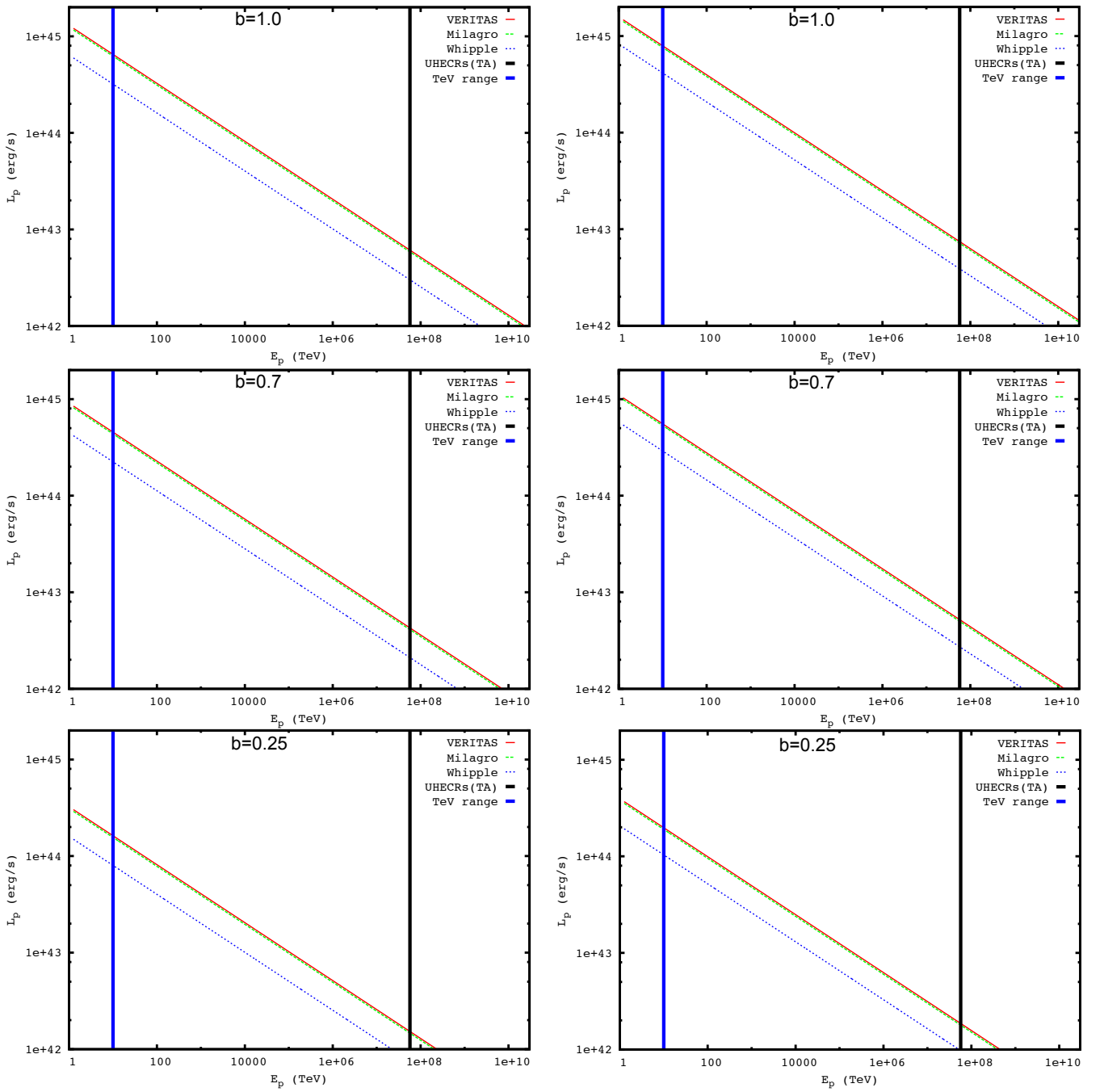

FIG. 4.— Proton luminosity as a function of its energy is plotted. The values of proton luminosity are normalized with the TeV γ-ray observations of Mrk 421. In this figure we highlight two zones; the blue solid line represents those protons responsible for the TeV γ production around $E_{\nu,\rm pk} \simeq 10$ TeV and the black solid line represents those with energy collected in TA experiment. We consider the values of photon flux normalization fitted with a simple power law (left) and a power law with exponential cutoff (right) for b=1.0 (top), b-=0.7 (middle) and b=0.25 (bottom).